

# Simulation and analysis of electron cyclotron resonance discharges

M. Ardehali

Research Laboratories, NEC Corporation,  
Sagamihara, Kanagawa 229 Japan

## Abstract

We describe in detail the method for Particle-in cell/Monte-Carlo simulation of electron cyclotron resonance (ECR) discharges. In the simulation, electric and magnetic fields are obtained by solving Maxwell equations, and electrons and ions are accelerated by solving equations of motion. We consider two different cases: (i) propagation of electromagnetic wave in the presence of a constant external magnetic field; (ii) propagation of electromagnetic wave in the presence of a linearly decreasing magnetic field which corresponds to a realistic ECR discharge. The simulation results indicate that at the resonance layer, the electrons are heated by the electromagnetic wave, and the incoming wave amplitude is pronouncedly damped, with the wave hardly propagating through the ECR layer.

In recent years, there has been increasing interest in high density plasmas at low gas pressures for semiconductor wafer processing [1]. Unlike Reactive Ion Etching (RIE) discharges in which the electrons mean free path is of order of a few centimeters, in Electron Cyclotron Resonance (ECR) discharges, the electrons are confined by the external magnetic field and their mean free path is of order of less than a millimeter. Thus ECR discharges are capable of generating high density plasmas at low gas pressures and low temperatures. Because of these advantages, numerous experiments have been performed to study these discharges. However, the fundamental understanding of these discharges is not yet satisfactory. The main goal of this work is to describe the method for simulating ECR discharges using the self consistent Particle-in-cell/Monte-Carlo (PIC/MC) technique.

The present PIC/MC simulator uses particle-in-cell (PIC) scheme for charge-assignment-force-interpolation [2], and Monte Carlo technique for collisions and scatterings. In the simulation, an electromagnetic wave with frequency  $\omega_0 = 2.45$  GHz enters the system along the  $z$  axis. PIC/MC is used to model the interaction of the electromagnetic wave with the electrons and ions.

Very briefly, the PIC/MC algorithm for ECR plasma consists of the following five subroutines:

(I) Interpolate the instantaneous velocities of MC particles representing ions and electrons to the grid points using PIC technique. Once the velocity of ions and electrons at a grid is obtained, the current density at the same grid can easily be calculated.

(II) Solve the Maxwell's equation on a spatially discretized mesh to obtain the electric and magnetic fields. In the simulation, we assume that the electric and magnetic fields do not vary along the  $x$  and  $y$  axes, i.e., we only consider  $E_x(z, t)$ ,  $E_y(z, t)$ ,  $E_z(z, t)$ ,  $B_x(z, t)$ ,  $B_y(z, t)$ ,  $B_z(z, t)$ . This assumption is justifiable since electrons are confined to a radius of less than a millimeter by the external magnetic field. For example, for an electron temperature of 2 eV, which corresponds to the electron velocity of  $10^8$  cm/sec, and for a magnetic field of  $B = 10^{-2}$  T, the electron's radius is less than 1 millimeter (here we have used the formula  $r = \frac{m|v|}{eB \sin \phi}$ , here  $\phi$  is the angle between the momentary electron velocity vector and the magnetic field vector, and  $|v|$  is the absolute value of the electron velocity).

Assuming the electric and magnetic fields do not have any variations along the  $x$  and  $y$  directions, the Maxwell's equations can be written as

$$\frac{\delta E_x}{\delta t} = -c \frac{\delta B_y}{\delta z} - 4\pi J_x \quad (1)$$

$$\frac{\delta B_y}{\delta t} = -c \frac{\delta E_x}{\delta z}, \quad (2)$$

$$\frac{\delta E_y}{\delta t} = c \frac{\delta B_x}{\delta z} - 4\pi J_y, \quad (3)$$

$$\frac{\delta B_x}{\delta t} = c \frac{\delta E_y}{\delta z}, \quad (4)$$

$$\frac{\delta E_z}{\delta t} = -4\pi J_z, \quad (5)$$

$$\frac{\delta B_z}{\delta t} = 0. \quad (6)$$

In the above equations,  $E$ 's,  $B$ 's and  $J$ 's represent the electric field and magnetic

field and current density. The boundary conditions are obtained by assuming that the circularly polarized waves enter the plasma from the left and that the transverse waves leave the system without being reflected. Thus the horizontal and vertical components of the electric and magnetic fields at  $z = 0$  and  $z = L$  are given by

$$\begin{aligned} E_x(0) &= E_0 \cos \omega t, & B_x(0) &= B_0 \sin \omega t, & E_y(0) &= E_0 \sin \omega t, & B_y(0) &= -B_0 \cos \omega t, \\ E_x(L) &= 0, & B_x(L) &= 0, & E_y(L) &= 0, & B_y(L) &= 0, \end{aligned} \quad (7)$$

where  $\omega$  is the frequency of the source, and  $E_0$  and  $B_0$  are the electric and magnetic field of the source, i.e., the electric and magnetic field at  $z = 0$ . The boundary condition of the longitudinal electric field is obtained by solving Gauss Equations, i.e.,

$$E_z(0) = 4\pi\sigma(0, t), \quad E_z(L) = 4\pi\sigma(L, t), \quad (8)$$

where  $\sigma(0, t)$  and  $\sigma(L, t)$  are the surface charge density at the left and right boundaries which vary with time. The surface charge density can be obtained from

$$\begin{aligned} \sigma(0, t) &= \int_0^t (J_i(0) - J_e(0)) dt', \\ \sigma(L, t) &= \int_0^t (J_i(L) - J_e(L)) dt'. \end{aligned} \quad (9)$$

The longitudinal boundary conditions imply that the total charge of the system including the boundaries is zero.

The Maxwell's equation for the transverse wave is obtained by adding and subtracting Eqs. 1 and 2 (or Eqs. 3 and 4), i.e.,

$$\begin{aligned} \left( \frac{\delta}{\delta t} + c \frac{\delta}{\delta z} \right) F_{x;y} &= -4\pi J_{x;y}, \\ \left( \frac{\delta}{\delta t} - c \frac{\delta}{\delta z} \right) G_{x;y} &= -4\pi J_{x;y}, \end{aligned} \quad (10)$$

where  $F_x = E_x + B_y$ ,  $G_x = E_x - B_y$ ,  $F_y = E_y + B_x$ , and  $G_y = E_y - B_x$ . Note that the left-hand side of Eq. (10) can be considered as the total derivative along the vacuum line  $z = ct$ . Thus if we assume  $\Delta z = c\Delta t$ , Eq. (10) may be discretized as [3]

$$\frac{F_{x;y}(t + \Delta t, z + c\Delta t) - F_{x;y}(t, z)}{\Delta t} = -4\pi J_{x;y} \left( t + \frac{\Delta t}{2}, z + c \frac{\Delta t}{2} \right), \quad (11)$$

or

$$F_{x;y,j+1}^{n+1} = F_{x;y,j}^n - 4\pi [(J_{x;y,j+1} + J_{x;y,j}) / 2] \Delta t. \quad (12)$$

Thus the summation of the  $x$  component of the electric field and the  $y$  component of the magnetic field at grid point  $j + 1$  and at the time  $n + 1$  depends on the summation of the  $x$  component of the electric field and the  $y$  component of the magnetic field at grid point  $j$  and at the time  $n$  and on the average current

density between grids  $j$  and  $j + 1$  at time  $t + \Delta t/2$ . Using the above technique, one can obtain  $E_x(z, t), E_y(z, t), B_x(z, t)$ , and  $B_y(z, t)$ .

(III) Interpolate the electric field and the magnetic field from the grid points to the location of particles. Once the electric and magnetic fields at the location of particles are known, equations of motion can be solved.

(IV) Integrate the equations of motion under the local and instantaneous electric and magnetic fields. To move the particles, we have to solve Lorentz equation.

$$\mathbf{v}^{n+1} = \mathbf{v}^n + \frac{q}{m} \Delta t \left[ \mathbf{E}^n + \frac{1}{2} (\mathbf{v}^{n+1} + \mathbf{v}^n) \times \mathbf{B}^n \right] - \Delta t \frac{g}{m} \frac{\Delta \mathbf{B}_{ext}}{\Delta z}, \quad (13)$$

where  $g$  is the magnetic moment and  $\mathbf{B}_{ext}$  is the external magnetic field. Note that the simulation uses Leap-Frog technique, and hence time  $n$  refers to  $t - \Delta t/2$  and time  $n + 1$  refers to  $t + \Delta t/2$ .

Since  $\mathbf{v}^{n+1}$  appears on both sides of the above equation, one has to proceed very carefully. To obtain the velocity at time  $n + 1$  from the velocity at time  $n$ , we use Boris's technique [4], which is based on the following three steps:

(i) First we define velocity  $\mathbf{v}^-$  as

$$\mathbf{v}^- = \mathbf{v}^n + \frac{q\mathbf{E}}{m} \frac{\Delta t}{2} - \frac{g}{m} \frac{\Delta \mathbf{B}_{ext}}{\Delta z} \frac{\Delta t}{2} \quad (14)$$

Next we define velocity  $\mathbf{v}'$  which is related to the velocity  $\mathbf{v}^-$  by the following relation

$$\mathbf{v}' = \mathbf{v}^- + \mathbf{v}^- \times \mathbf{r}, \quad (15)$$

where the function  $\mathbf{r}$  is defined as  $\mathbf{r} = \frac{q\mathbf{B}}{m} \frac{\Delta t}{2}$ .

(iii) Finally we define velocity  $\mathbf{v}^+$

$$\mathbf{v}^+ = \mathbf{v}^- + \mathbf{v}' \times \mathbf{s} \quad (16)$$

where the function  $\mathbf{s}$  is defined as

$$\mathbf{s} = \frac{2\mathbf{r}}{1 + |\mathbf{r}|^2} \quad (17)$$

Boris [4] has shown that the velocity at time  $t + \Delta t$  can be obtained from the following equation

$$\mathbf{v}^{n+1} = \mathbf{v}^+ + \frac{q\mathbf{E}}{m} \frac{\Delta t}{2} - \frac{g}{m} \frac{\Delta \mathbf{B}_{ext}}{\Delta z} \frac{\Delta t}{2} \quad (18)$$

The equations of motions for electrons and ions at time  $t$  is numerically integrated to obtain the position of the electrons and ions at time step  $t + \Delta t$ .

$$z(t + \Delta t) = z(t) + \mathbf{v}^{n+1} \Delta t \quad (19)$$

(V) Use random numbers (Monte Carlos technique) and collision cross sections to account for scattering and ionizations. The total electron-neutral scattering cross section  $\sigma_{total}(v)$  is  $\sigma_{total}(v) = \frac{K_{total}}{v}$ , where  $v$  is the electron velocity and  $K_{total} = 2 \times 10^{-8} \text{ cm}^3/\text{s}$  is the rate constant. Ionizing collisions occur if the electron energy is larger than a specific value (for example, for Argon the

threshold energy is 15 eV). An ionizing collision is modeled by loading a new electron and ion at the position of the ionizing electron. The kinetic energy after ionizing collision is partitioned between the two electrons. Ion-ion charge exchange and ion-ion elastic collisions are also included in the simulator.

In the simulator, the charged particles move under the influence of the self-consistent electric and magnetic fields and suffer collisions with neutral particles. The neutral gas density is chosen to be  $2 \times 10^{-14} \text{cm}^{-3}$ . The size of the discharge is 24 cm and the number of grids is 2667. Microwave with an amplitude of 0.16 Gauss and at a frequency of 2.45 GHz enters the system from the left along the  $z$  axis and propagates through the discharge.

Figure 1 (a) [Fig. 1 (b)] shows the variations of  $E_x, E_y$  [ $B_x, B_y$ ] within the discharge in the absence of particles. The incoming wave propagates through the discharge without attenuation. These figures clearly demonstrate that the subroutine solving Maxwell equation is working properly.

We now consider the coupling of the electro-magnetic wave to the electrons and ions. First, we briefly describe the fundamental principles of the ECR discharges. We consider an external magnetic field along the  $z$  axis with a magnitude of  $B_{ext}$  (for simplicity we assume that the external electric field is zero). An electron rotates around the magnetic field with a frequency of  $\omega_c = \frac{qB_{ext}}{mc}$  ( $\omega_c$  is 2.45 GHz when the external magnetic field is  $B_{ext} = 875$  Gauss). We now assume that an electromagnetic wave with frequency  $\omega_0$  enters this system. If  $\omega_0$  is much smaller or much larger than  $\omega_c$ , the electron is not heated by the incoming wave. However, when  $\omega_0 = \omega_c$ , resonance condition is attained and the wave energy is absorbed, leading to strong acceleration of electrons.

In the simulation, we assume an electromagnetic wave with frequency  $\omega_0 = 2.45$  GHz enters the system from the left. First we consider two types of external magnetic fields: (1)  $B_{ext} = 1875$  G which corresponds to an electron cyclotron frequency of  $\omega_c = \frac{qB_{ext}}{mc} = 5.24 \text{GHz}$ , (2)  $B_{ext} = 875$  G which corresponds to an electron cyclotron frequency of  $2.45 \text{GHz}$ . Figure 2 (a) [Figure 2 (b)] shows the variation of the horizontal component of the electric [magnetic] field within the discharge. When  $B_{ext} = 875$  G, which corresponds to electron cyclotron frequency of 2.45 GHz and which is equal to the frequency of the electromagnetic wave, resonance occurs and the electric and magnetic fields of the incoming electromagnetic wave are pronouncedly damped, with the wave hardly propagating within the discharge. In contrast, when  $B_{ext} = 1875$  G, which corresponds to an electron cyclotron frequency of 5.25 GHz and which is much larger than the frequency of the incoming wave, the electric and magnetic fields of the electromagnetic wave propagate through the discharge without attenuation (note that we use CGS system where both electric and magnetic fields are measured in Gauss).

Figure 3 shows the horizontal component of electron velocity within the discharge. When  $B_{ext} = 875$  G, resonance occurs and the electrons are heated by the incoming electromagnetic wave. Thus the horizontal component of the electron velocity increases sharply right at the boundary. However, When  $B_{ext} = 1875$  G, the electrons do not absorb much energy from the incoming wave. The electron velocity is therefore small at the boundary and does not change rapidly within the discharge.

In the previous examples, we assumed that the external magnetic field is constant within the discharge. In an actual ECR discharge,  $B_{ext}$  drops along  $z$

axis. To model a realistic ECR discharge [5], we simulated a system where the external magnetic field decreases linearly along the  $z$  axis so that at the center of the discharge, the external magnetic field is 875 G and hence resonance occurs.

Figs. 4 (a) and 4 (b) show the trajectories of electrons at the center of discharge when the external magnetic fields of 1875 G and 875 G. Although in the simulation, we trace the electrons only along the  $z$  direction, Figs. 4 (a) and 4 (b) are obtained by integrating  $V_x$  and  $V_y$  over time. Note that when  $B_{ext} = 875$  G, i.e., when  $\omega_c = \omega_0$ , resonance condition is attained and electrons spiral around the external magnetic field. In contrast, when  $B_{ext} = 1875$  G, i.e., when  $\omega_c \gg \omega_0$ , resonance does not occur and electrons do not spiral around the magnetic field.

Figures 5(a) and 5(b) show the horizontal and vertical components of the electric field within the discharge. The incoming electromagnetic wave is entirely absorbed by the electrons near the resonance layer, with both  $E_x$  and  $E_y$  dropping rapidly near the ECR layer. The incoming wave hardly propagates beyond the resonance layer.

Figures 6(a) and 6(b) show the horizontal and vertical components of the electron velocity within the discharge after 65 cycles. At the resonance layer, the velocity of electrons jumps significantly, indicating that the electrons absorb considerable energy from the incoming electromagnetic wave. However at other positions within the discharge, the velocity of electrons does not change rapidly, indicating that the electrons absorb very little energy. Of course after many cycles, the horizontal and vertical components of electron velocity become isotropic as the the electrons localized near the resonance layer create new electrons by ionization as well as diffusing toward the boundaries. To clearly demonstrate the heating of the electrons at the resonance layer, we present here the simulation results after only 65 cycles.

In summary, PIC/MC technique has been used to investigate the fundamental properties of an electropositive ECR discharge. The simulation results indicate that at resonance layer, i.e., at  $\omega_c = \omega_0$ , the incoming electromagnetic wave is pronouncedly damped, leading to dramatic acceleration of electrons. The simulation results also show that at resonance layer, electrons spiral around the external magnetic field. PIC/MC technique shows great promise for simulating more complex (for example electronegative) discharges in two or three dimensions.

## References

- [1] W. M. Holber and J. Forster, *J. Vac. Sci. Technol. A* 8, 3720 (1990); M. A. Lieberman and R. A. Gottscho, "Design of high density plasma sources for material processing," in *Physics of Thin Films*, M. Francombe and J. Vossen, Eds. New York: Academic, 1993.
- [2] R. Hockney and J. Eastwood, *Computer simulation using particles* (McGraw-Hill, New York, 1981).
- [3] C. K. Birdsall and A. B. Langdon, *Plasma Physics Via Computer Simulation* (McGraw-Hill, New York, 1985).
- [4] J. P. Boris, *Proceeding of the Fourth Conference on Numerical Simulations on Plasmas*, Naval Research Laboratory, Washington, D.C., 3-67, November 1970.
- [5] W. H. Koh, N. H. Choi, D. I. Choi, and Y. H. Oh, *J. Appl. Phys.* 73, 4205 (1993).

## Figure Captions

### IMPORTANT NOTE:

Figs. 1 (a) and 1 (b) are on the same page.

Figs. 2 (a) and 2 (b) are on the same page.

Figure 3 is on one page.

Figs. 4 (a) and 4 (b) are on the same page.

Figs. 5 (a) and 5 (b) are on the same page.

Figs. 6 (a) and 6 (b) are on the same page.

Fig. 1 (a) Profile of the horizontal (solid line) and vertical (dashed line) components of the electric field within the discharge in the absence of particles.

Fig. 1 (b) Profile of the horizontal (solid line) and vertical (dashed line) components of the magnetic field within the discharge in the absence of particles.

Fig. 2 (a) Profile of the horizontal component of the electric field within the discharge when the external magnetic field is at 875 G (solid line) and at 1875 G (dashed line).

Fig. 2 (a) Profile of the horizontal component of the magnetic field within the discharge when the external magnetic field is at 875 G (solid line) and at 1875 G (dashed line).

Fig. 3 Profile of the horizontal component of electron velocity within the discharge when the external magnetic field is at 875 G (solid line) and at 1875 G (dashed line).

Fig. 4 (a) Trajectories of electrons when the external magnetic field is at 1875 Gauss.

Fig. 4 (a) Trajectories of electrons when the external magnetic field is at 875 Gauss.

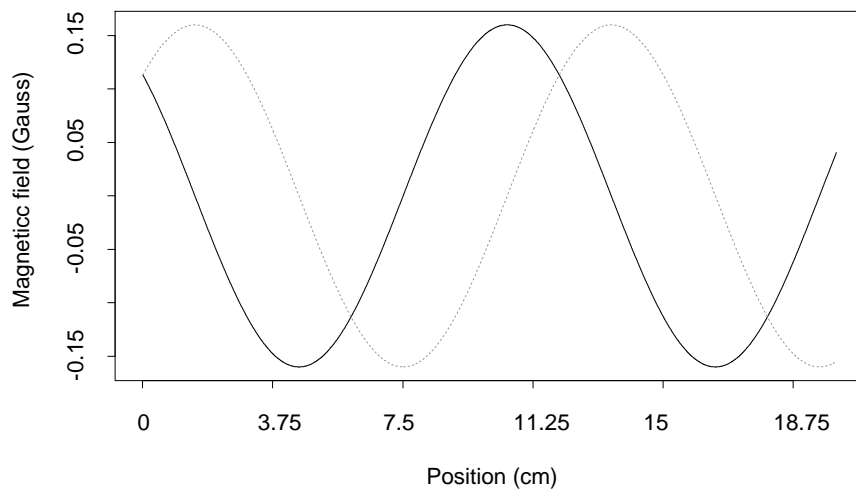
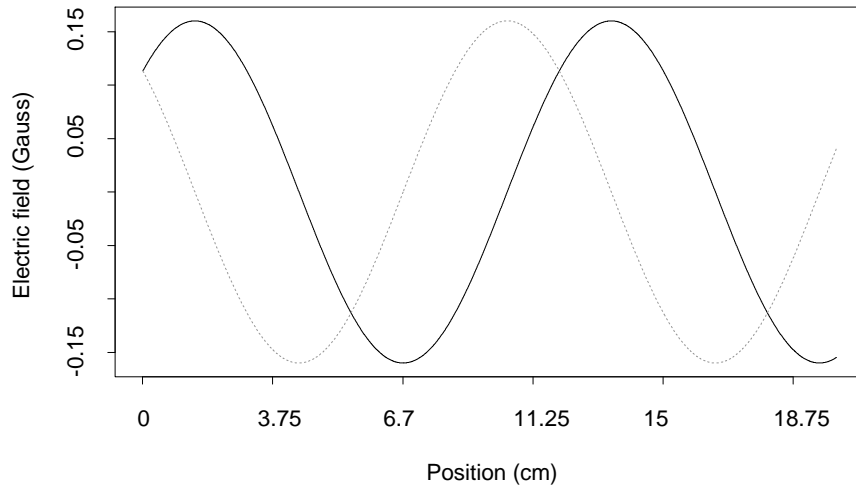
Fig. 5 (a) Profile of the horizontal component of electric field in an ECR discharge. Note that at the center of the discharge, the external magnetic field is 875 G.

Fig. 5 (b) Profile of the vertical component of electric field in an ECR discharge.

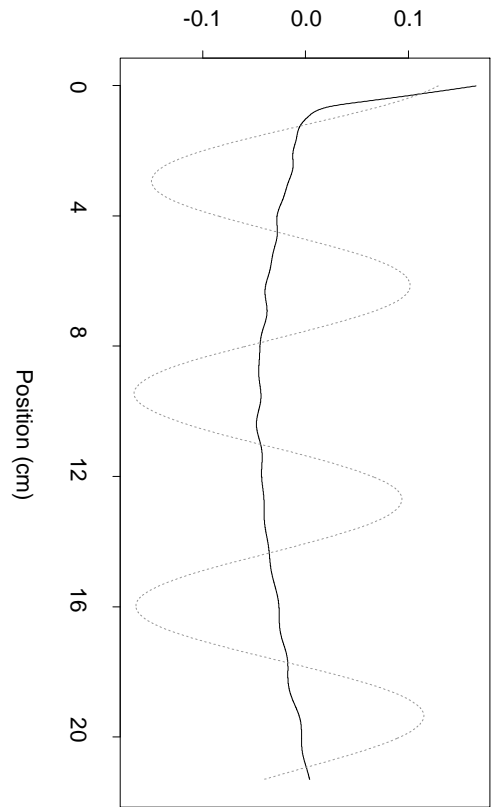
Fig. 6 (a) Profile of the horizontal component of electron velocity in an ECR discharge after 65 cycles.

Fig. 6 (b) Profile of the vertical component of electron velocity in an ECR discharge after 65 cycles.





Horizontal component of the electric field (Gauss)



Horizontal component of the magnetic field (Gauss)

